Environmental Research Letters

LETTER • OPEN ACCESS

A connection from Arctic stratospheric ozone to El Niño-Southern oscillation

IOP Publishing Environ. Res. Lett. 11 (2016) 124026 doi:10.1088/1748-9326/11/12/124026

Environmental Research Letters

OPEN ACCESS

RECEIVED
10 July 2016

REVISED
28 November 2016

ACCEPTED FOR PUBLICATION
29 November 2016

PUBLISHED
14 December 2016

LETTER

A connection from Arctic stratospheric ozone to El Niño-Southern oscillation

Fei Xie[1], Jianping Li[1], Wenshou Tian[2], Qiang Fu[3], Fei-Fei Jin[4], Yongyun Hu[5], Jiankai Zhang[2], Wuke Wang[6], Cheng Sun[1], Juan Feng[1], Yun Yang[2] and Ruiqiang Ding[7]

1 College of Global Change and Earth System Science, Beijing Normal University, Beijing, People's Republic of China
2 College of Atmospheric Sciences, Lanzhou University, Lanzhou, People's Republic of China
3 Department of Atmospheric Sciences, University of Washington, Seattle, WA, USA
4 Department of Meteorology, University of Hawaii at Manoa, Honolulu, Hawaii, USA
5 Department of Atmospheric and Oceanic Sciences, School of Physics, Peking University, Beijing, People's Republic of China
6 Institute for Climate and Global Change Research, School of Atmospheric Sciences, Nanjing University, Nanjing 210023, People's Republic of China
7 State Key Laboratory of Numerical Modeling for Atmospheric Sciences and Geophysical Fluid Dynamics, Institute of Atmospheric Physics, Chinese Academy of Sciences, Beijing, People's Republic of China

E-mail: ljp@bnu.edu.cn

Keywords: Arctic stratospheric ozone (ASO), ENSO, NPO, Victoria Mode

Abstract

Antarctic stratospheric ozone depletion is thought to influence the Southern Hemisphere tropospheric climate. Recently, Arctic stratospheric ozone (ASO) variations have been found to affect the middle-high latitude tropospheric climate in the Northern Hemisphere. This paper demonstrates that the impact of ASO can extend to the tropics, with the ASO variations leading El Niño-Southern Oscillation (ENSO) events by about 20 months. Using observations, analysis, and simulations, the connection between ASO and ENSO is established by combining the high-latitude stratosphere to troposphere pathway with the extratropical to tropical climate teleconnection. This shows that the ASO radiative anomalies influence the North Pacific Oscillation (NPO), and the anomalous NPO and induced Victoria Mode anomalies link to the North Pacific circulation that then influences ENSO. Our results imply that incorporating realistic and time-varying ASO into climate system models may help to improve ENSO predictions.

1. Introduction

Stratospheric ozone is not only vital to protecting life on Earth, as it absorbs harmful solar ultraviolet radiation (Lubin and Jensen 2002, Chipperfield *et al* 2015), but also essential to the control of the stratospheric temperature via atmospheric radiative heating. The latter influences the circulation and chemical composition of the stratosphere (Haigh 1994, Ramaswamy *et al* 1996, Forster and Shine 1997), and can also affect tropospheric weather and climate (Baldwin and Dunkerton 2001, Graf and Walter 2005, Ineson and Scaife 2009, Cagnazzo and Manzini 2009, Reichler *et al* 2012, Karpechko *et al* 2014, Kidston *et al* 2015, Zhang *et al* 2016).

Antarctic stratospheric ozone has decreased over the past 60 years in association with anthropogenic emissions of ozone depleting substances (Solomon 1990, 1999, Ravishankara *et al* 1994, 2009). The Antarctic ozone hole is thought to influence the Southern Hemisphere tropospheric climate (Son *et al* 2008, Feldstein 2011, Kang *et al* 2011, Thompson *et al* 2011, Gerber and Son 2014, Waugh *et al* 2015). However, the situation in the Arctic is markedly different. The multi-decadal Arctic ozone loss has been much smaller than that of Antarctic ozone (World Meteorological Organization (WMO) 2011) because the winter/spring Arctic polar cap is warmer than the Antarctic polar cap. Thus, the Northern Hemisphere surface climate response to Arctic ozone loss is less evident (e.g., Thompson and Solomon 2005). In contrast, the year-to-year variability of the Arctic stratospheric temperature is much larger than that of the Antarctic stratospheric temperature (Randel 1988), owing to frequent 'sudden warming' events (Charlton and Polvani 2007) in the Arctic stratosphere caused by the abundance of planetary scale waves that propagate into the Arctic stratosphere and perturb the circulation there. The amplitude of the interannual variability in Arctic ozone is comparable with, or even much larger than, that in Antarctic ozone (Manney *et al* 2011).

Cheung *et al* (2014) and Karpechko *et al* (2014) used the UK Met Office operational weather forecasting system and the atmospheric circulation model ECHAM5, respectively, to explore the possible surface impacts associated with extreme Northern Hemisphere ozone anomalies. They concluded that stratospheric ozone changes alone did not appear to have a significant effect on surface conditions. More recently, Arctic stratospheric ozone (ASO) variations have been found to cause Northern Hemisphere mid-high latitude tropospheric circulation and sea level pressure (SLP) anomalies. Smith and Polvani (2014) and Calvo *et al* (2015) performed numerical experiments that showed a statistically significant Northern Hemisphere mid-high latitude surface response to high and low values of synthetic ASO.

However, it is not known whether the impact of ASO extends to the tropics, for example, to influence the El Niño-Southern Oscillation (ENSO), a major climatic mode of tropical variability (e.g., Jin 1996, Timmermann *et al* 1999, Ashok and Yamagata 2009, Latif and Keenlyside 2009, Yeh *et al* 2009) that has great global climatic and societal impacts (e.g., Orlove *et al* 2000, McPhaden *et al* 2006, Deser *et al* 2010). It is well known that ENSO can influence tropical ozone through anomalous convection (Camp *et al* 2003, Xie *et al* 2014) and the high-latitude stratospheric ozone (Brönnimann *et al* 2004, Eyring *et al* 2006, Cagnazzo *et al* 2009, Zhang *et al* 2015) through anomalous propagation and dissipation of ultra-long Rossby waves at mid-latitudes (Gettelman *et al* 2001, Calvo *et al* 2004, Manzini *et al* 2006, Garfinkel and Hartmann 2008, Randel *et al* 2009, Hurwitz *et al* 2011, Xie *et al* 2012, 2014). Figure 1 shows the lead–lag correlation coefficients at three-monthly intervals between the ENSO index and zonally averaged ozone, for ENSO variations leading ozone by 3 months to lagging ozone by 24 months. We see that, as expected, ENSO has significant correlations with tropical and high latitude stratospheric ozone when ENSO leads ozone by three months. However, figure 1 also shows an unexpected result: ENSO is significantly correlated with ASO when ENSO lags ozone by 20 months. This implies that changes in ASO may cause a later change in ENSO. The aim of this study is to explain why this happens.

2. Data, methods, and simulations

Figure 1(i) shows that the region where ozone has a good leading correlation with the ENSO index is limited to approximately 60–90°N and 150–50 hPa, and this is the area where the variability and depletion of ozone concentration is most pronounced in the Northern Hemisphere (Manney *et al* 2011). The monthly anomaly of ozone concentration (after removing the climatological mean seasonal cycle), averaged over this region, is defined as the ASO index. Ozone values were obtained from the Stratospheric Water and OzOne Satellite Homogenized (SWOOSH, version 2.5, 1984–2015) dataset (Davis *et al* 2016), which is in good agreement with the ozone values (figure 2; $r = 0.89$) given by the Global Ozone Chemistry and Related trace gas Data Records for the Stratosphere (GOZCARDS, 1979–2012) project (Froidevaux *et al* 2015). The NASA Modern Era Retrospective Analysis for Research and Applications (MERRA) ozone is also used. It is in well in agreement with SWOOSH and GOZCARDS ozone (figure 2).

Sea surface temperature (SST) and SLP data were obtained from the UK Met Office Hadley Centre for Climate Prediction and Research SST (HadSST) and SLP (HadSLP) field datasets, respectively. Geopotential height and zonal wind were obtained from the National Centers for Environmental Prediction-Department of Energy (NCEP-DOE) dataset (version 2), and temperature data were taken from the Radiosonde Innovation Composite Homogenization (RICH) dataset (Haimberger *et al* 2008).

We calculated the statistical significance of the correlation between two auto-correlated time series using the two-tailed Student's *t*-test and the effective number (N^{eff}) of degrees of freedom (Bretherton *et al* 1999). For this study, N^{eff} was determined by the following approximation (Li *et al* 2012, 2013):

$$\frac{1}{N^{\mathrm{eff}}} \approx \frac{1}{N} + \frac{2}{N}\sum_{j=1}^{N}\frac{N-j}{N}\rho_{XX}(j)\rho_{YY}(j),$$

where N is the sample size, and ρ_{XX} and ρ_{YY} are the autocorrelations of two sampled time series, X and Y, respectively, at time lag j.

We used the National Center for Atmospheric Research's Community Earth System Model (CESM), version 1.0.6, which is a fully coupled global climate model that incorporates an interactive atmosphere (CAM/WACCM) component, ocean (POP2), land (CLM4), and sea ice (CICE). For the atmospheric component, we used the Whole Atmosphere Community Climate Model (WACCM), version 4 (Marsh *et al* 2013). WACCM4 is a climate model that has detailed middle-atmosphere chemistry and a finite volume dynamical core, and it extends from the surface to approximately 140 km. For our study, we disabled the interactive chemistry. WACCM4 has 66 vertical levels, with a vertical resolution of about 1 km

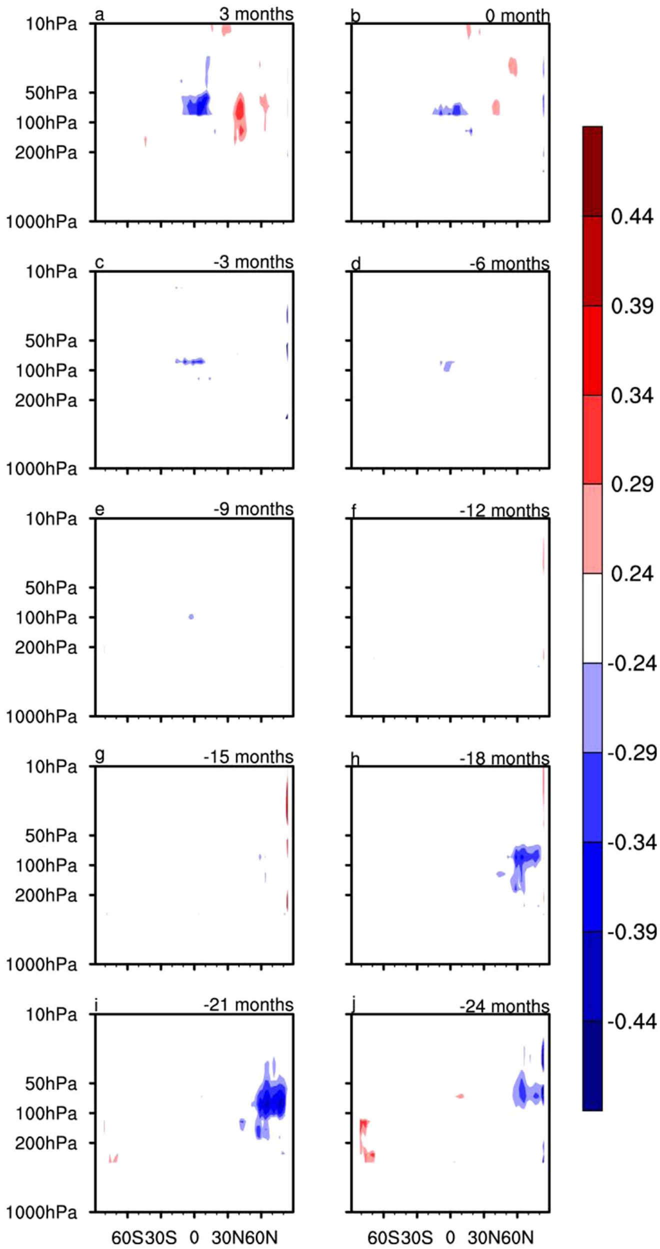

Figure 1. Correlation coefficients between the ENSO index and zonally averaged ozone, when the ENSO index leads ozone by (a) 3 months, (b) 0 months, (c) −3 months… and (j) −24 months. Ozone is based on SWOOSH data. ENSO is from the NINO3.4 index compiled by the Climate Prediction Center/NOAA. Only regions above the 95% confidence level are shown (see section 2 for the statistical significance test).

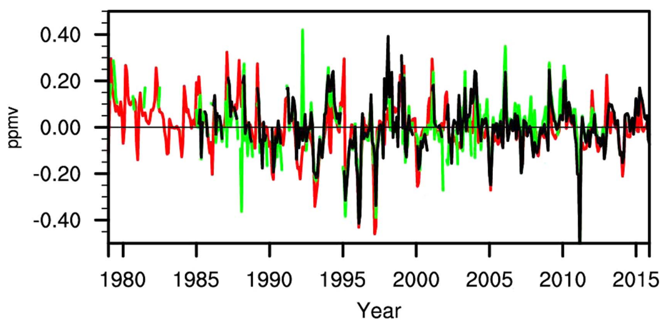

Figure 2. ASO represented by a time series of ozone averaged over the region 60°–90°N at 150–50 hPa from SWOOSH ozone (black line), GOZCARDS ozone (green line), and MERRA ozone (red line).

Table 1. Fully coupled CESM–WACCM4 experiments with various specified ozone forcings.

Experiment[a]	Specified ozone forcings
E_1	Transient run using case B_1955–2005_WACCM_SC_CN in CESM. All natural and anthropogenic external forcings for E_1 based on original CESM input data. E_1 is a historical simulation covering the period 1955–2005. Note that the specified ozone forcing for 1955–2005 was derived from the CMIP5 ensemble mean ozone output. The specified ozone forcing was named ghg_forcing_1955-2005_CMIP5_EnsMean.c140414.nc, and can be downloaded at https://svn-ccsm-inputdata.cgd.ucar.edu/trunk/inputdata/atm/waccm/ub/ghg_forcing_1955-2005_CMIP5_EnsMean.c140414.nc.
E_2 E_3 E_4	All forcings and design are as E_1, except that the specified ozone forcing in the region 30°–90°N, at 300–30 hPa[b] was replaced by MERRA ozone data for the period 1979–2005. Ozone outside of the region 30°–90°N, 300–30 hPa is the same as E_1. These are three ensemble simulations using slightly different initial conditions[c].

[a] Integration time for E_1 was 1955–2005 but 1979–2005 for $E_{2–4}$.

[b] To avoid the effect of the boundary of ozone change on the Arctic stratospheric circulation simulation, the replaced region (30°–90°N, 300–30 hPa) was larger than the region used to define the ASO index (60°–90°N, 150–50 hPa).

[c] To produce different initial conditions, the parameter ⟨pertlim⟩ was used in the CESM model, which produces an initial temperature perturbation. The magnitude was about e^{-14}.

in the tropical tropopause and lower stratosphere layers. Simulations used a horizontal resolution of 1.9° × 2.5° (latitude × longitude) for the atmosphere and approximately the same for the ocean.

Four transient experiments (E_1–E_4) with the fully coupled ocean incorporated both natural and anthropogenic external forcings, including spectrally resolved solar variability (Lean *et al* 2005), transient greenhouse gasses (GHGs) (from scenario A1B of IPCC 2001), volcanic aerosols (from the Stratospheric Processes and their Role in Climate Chemistry–Climate Model Validation (CCMVal) REF-B2 scenario recommendations), a nudged quasi-biennial oscillation (QBO) (the time series in CESM is determined from the observed climatology over the period 1955–2005), and specified ozone forcing derived from the CMIP5 ensemble mean ozone output. E_1 is a historical simulation covering the period 1955–2005. All forcings and design of E_2 are as E_1, except that the specified ozone forcing in the region 30–90°N, at 300–30 hPa was replaced by MERRA ozone data for the period 1979–2005. Ozone outside of the region 30–90°N, 300–30 hPa is the same as E_1. E_3 and E_4 are two ensemble simulations with E_2 using slightly different initial conditions. An overview of all coupled experiments is given in table 1. All of the forcing data used in this study are available from the CESM model input data repository.

3. A connection between the ASO and ENSO

To probe the relationship between the changes in ASO and ENSO over the past three decades, their lead–lag correlation is shown in figure 3(a). The correlation for ENSO leading the ASO by about three months is statistically significant. This agrees with previous studies showing that ENSO can affect Northern Hemisphere stratospheric ozone after 2–3 months, as the Rossby waves excited by ENSO reach the Northern Hemisphere mid-high latitudes and then move into the stratosphere (Manzini *et al* 2006, Fischer *et al* 2008, Cagnazzo *et al* 2009). A significant negative lagged correlation ($r = -0.35$, lag ca. 20 months) is also observed (figure 3(a)). This lagged correlation is further confirmed by figure 3(b), which shows time series of the ASO and ENSO indices, but with the time coordinate for ASO shifted forward by 20 months, representative of its observed lag. A spectrum analysis was performed on the changes in the ASO and ENSO indices (figures 3(c), (d)). There are similar low-frequency spectra in the 1–6 year band in the ASO and ENSO time series. To further establish the relationship between ENSO events and the ASO anomalies, figure 4(a) shows the scatter plot of winter ENSO events against the 20 month leading ASO anomalies. It illustrates that the strong El Niño/La Niña events correspond well to strong negative/positive ASO anomalies. Figure 4(b) pairs the winter NINO3.4 index and 20 month leading ASO index, giving a significant correlation coefficient of $r = -0.57$. The strong El Niño and strong La Niña events (e.g., 97/98, 15/16) since 1986 follow the strongly decreased and increased ASO anomalies that occurred about 20 months earlier.

To determine the connection between the ASO and the ENSO, we first examine the high-latitude stratosphere to troposphere pathway from the ASO to surface pressure variability. We find that the ASO is significantly correlated with the Arctic Oscillation and North Pacific Oscillation (NPO). A decrease in ASO radiatively cools the Arctic lower stratosphere (figure 5(a), green contour lines), which enhances the meridional temperature gradient in the lower stratosphere and thus strengthens stratospheric circulation (figure 5(a), black contour lines) via the thermal wind relationship. The stratospheric circulation anomalies in turn influence tropospheric circulation by the downward control principle (Haynes *et al* 1991) and tropospheric eddy momentum feedback (Kidston *et al* 2015). Geopotential height anomalies in the stratosphere propagate down to the surface (figure 5(a), color shading), resulting in an NPO-like signal over the North Pacific (figure 5(b)).

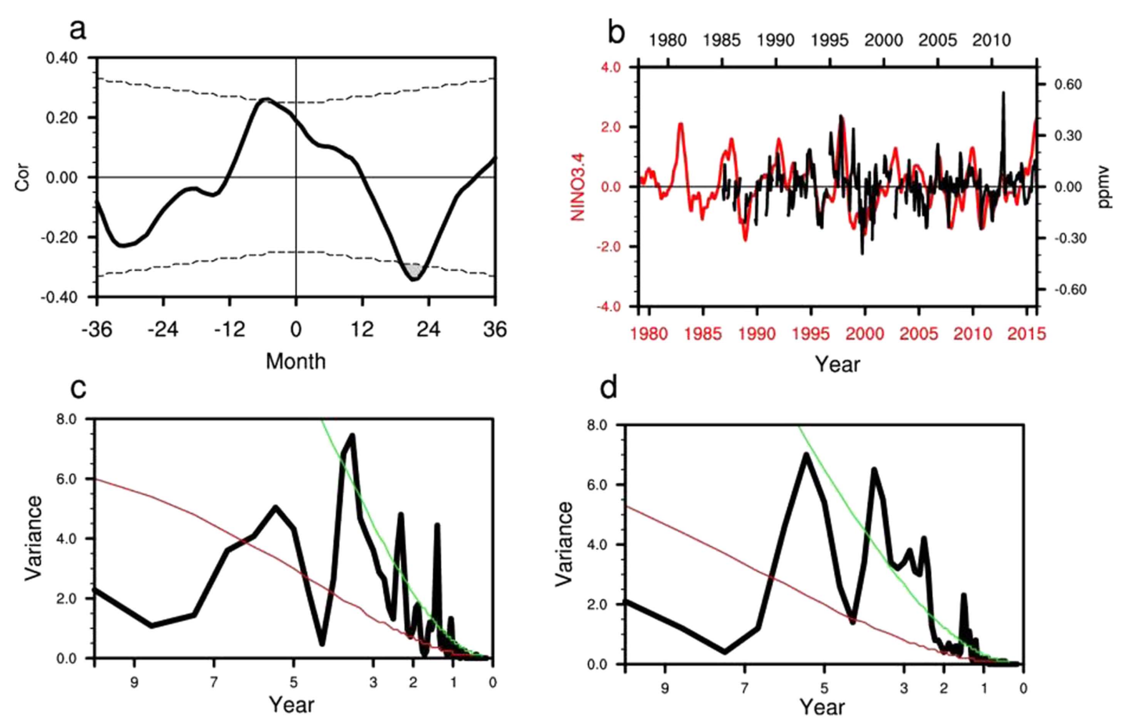

Figure 3. (a) Lead–lag correlation between the monthly ASO and ENSO indices; the ASO is a time series of ozone averaged over the region 60°–90°N at 150–50 hPa based on SWOOSH data; ENSO is from the NINO3.4 index compiled by the Climate Prediction Center/NOAA. The positive months on the x-axis refer to the ASO leading ENSO and negative months refer to ENSO leading the ASO; the dashed lines denote the 95% confidence level; the shaded areas indicate lead–lag correlations that are statistically significant. (b) ASO × −1 index (black line, 1984–2013) and ENSO index (1979–2015). The time coordinate for the ASO (upper one) is shifted forward by 20 months for a direct comparison. (c) Spectral analysis of ASO time series. The black line represents the spectral distribution. The green and red lines denote the 95% confidence level and the red noise spectrum, respectively. (d). Same as (c), but for the ENSO index.

Previous studies have demonstrated that the low-frequency variations of the Victoria Mode (VM; Bond *et al* 2003), which is similar to the North Pacific Gyre Oscillation (Di Lorenzo *et al* 2008), are effective in modulating the development of ENSO through the seasonal footprinting mechanism (Vimont *et al* 2001, Chen *et al* 2013, Ding *et al* 2015). This acts as an extra-tropical to tropical climate teleconnection via ocean–atmosphere dynamic interaction. The NPO-like signal is effectively linked to the VM anomalies (figure 6(a)). Thus, the extratropical to tropical climate teleconnection provides a link from the NPO/VM to ENSO through the following processes: North Pacific westerly anomalies generate SST and associated westerly anomalies through air–sea interaction in the subtropical central eastern North Pacific, central equatorial Pacific, and the western North Pacific. The latter alters the zonal SST gradient anomalies across the western central tropical Pacific (figure 6(b)), leading to westerly anomalies over the western central Pacific, which drive an El-Niño type event (Jin 1997a, 1997b; figures 6(c), (d)). The dynamic pathway and teleconnection from the ASO to the NPO, and from the NPO/VM to ENSO, together establish the ASO's connection to ENSO. Previous studies show that the NPO/VM lead ENSO by more than a year and a half (Ding *et al* 2015). Consequently, the ASO leads ENSO by about 20 months.

Note that a 35 month low-pass filter was applied to the ozone and SST data in figure 6. As described above, the lag panels in figure 6 reflect the seasonal footprinting mechanism. However, previous studies have demonstrated that only the low-frequency variations in VM are effective in modulating the development of ENSO through the seasonal footprinting mechanism (Vimont *et al* 2001, Ding *et al* 2015). On the other hand, a spectrum analysis was performed on the changes in the ASO and ENSO indices (figures 3(c), (d)). There are similar low-frequency spectra in the 1–6 year band in the ASO and ENSO time series. However, the low-frequency spectra in the 1–3 year band in both ASO and ENSO time series may be related to QBO. The 35 month low pass filter is used to filter out QBO effect on the lead–lag correlation between ASO and ENSO. This is why a 35 month low-pass filter is applied to the SST variations in figure 6. It would highlight the low-frequency variations, which are related to ozone changes, in the SST but remove noise-like high-frequency variations.

4. Simulated SST responses to ASO variations

North Pacific SST variability can influence the stratospheric polar vortex (Jadin *et al* 2010, Hurwitz

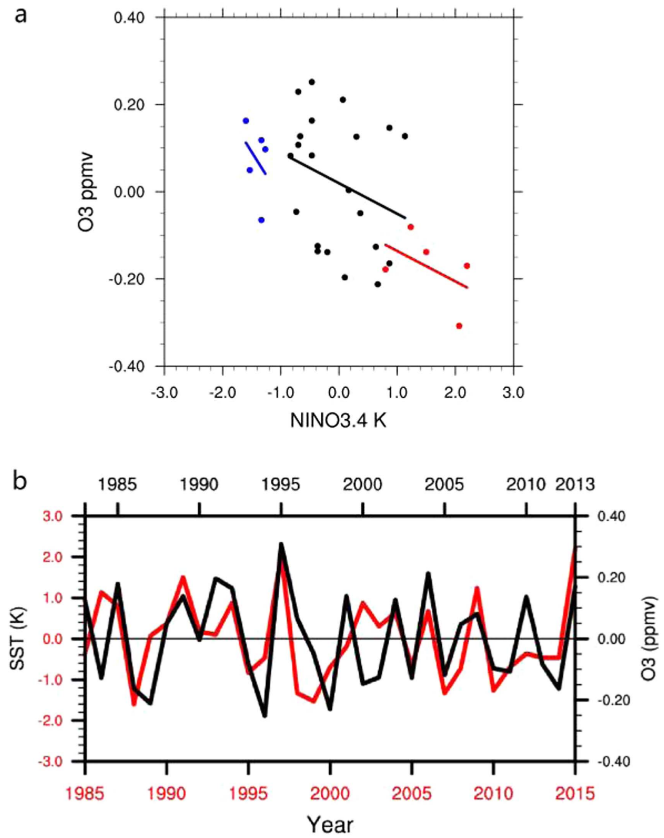

Figure 4. (a) The scatter plot of winter ENSO events versus 20 month leading ASO anomalies. Red spots represent the strong El Niño events (see table 2); blue spots are strong La Niña; black spots are neutral events. The lines represent the regression fit. ASO data are from MERRA; ENSO is from the NINO3.4 index compiled by the Climate Prediction Center/NOAA. (b) Winter ENSO index (red, 1986–2015) and 20 month leading ASO $\times -1$ index (black line). The time coordinate for the ASO (upper one) is shifted forward by 20 month for a direct comparison. The correlation coefficient is for the 20 month lead correlation (ASO leading ENSO).

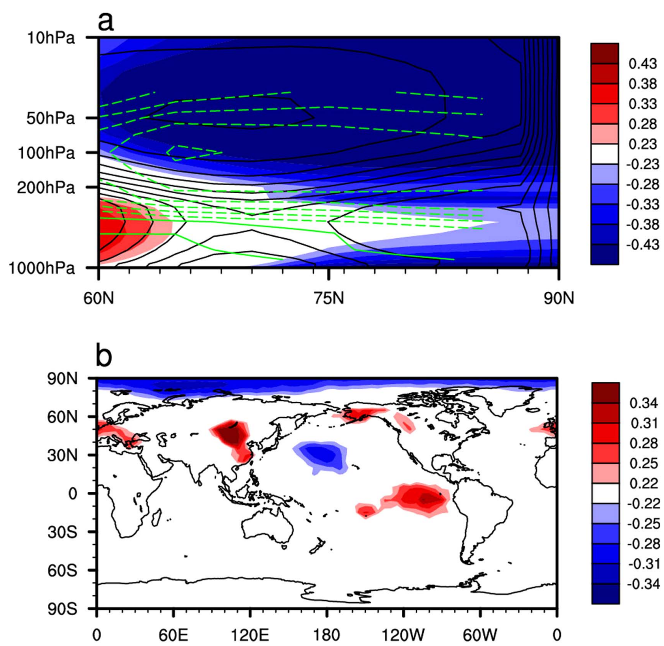

Figure 5. (a) Correlation coefficients between the ASO $\times -1$ and temperature (green contour lines), zonal wind (black contour lines), and geopotential height (color shading) for 1984–2015. Solid/dashed contour lines are at intervals of ± 0.2. (b) Correlation coefficients between the ASO $\times -1$ and SLP. Only regions above the 95% confidence level are colored. ASO data are from SWOOSH, geopotential height and zonal wind from NCEP2, temperature from RICH, and SLP from HadSLP.

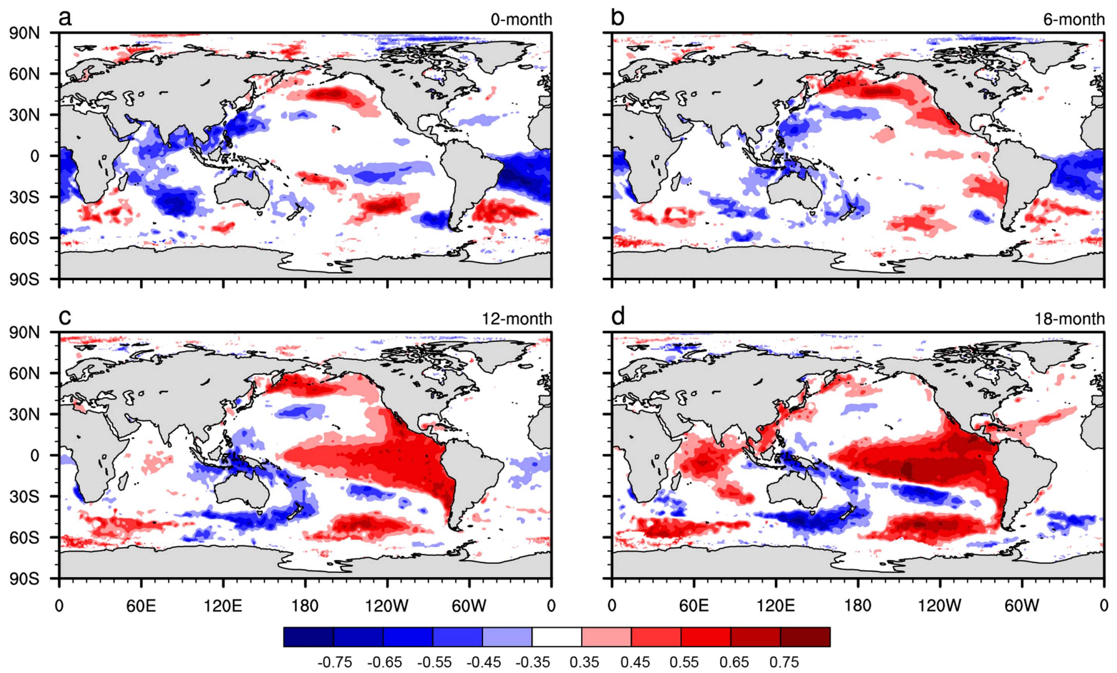

Figure 6. Correlation coefficients between the ASO×−1 and SST, when the ASO variations lead SST by (a) 0 months, (b) 3 months… and (h) 21 months, respectively. ASO data are from SWOOSH and SST from HadSST. Only regions above the 95% confidence level are colored. A 35 month low-pass filter was applied to ozone and SST.

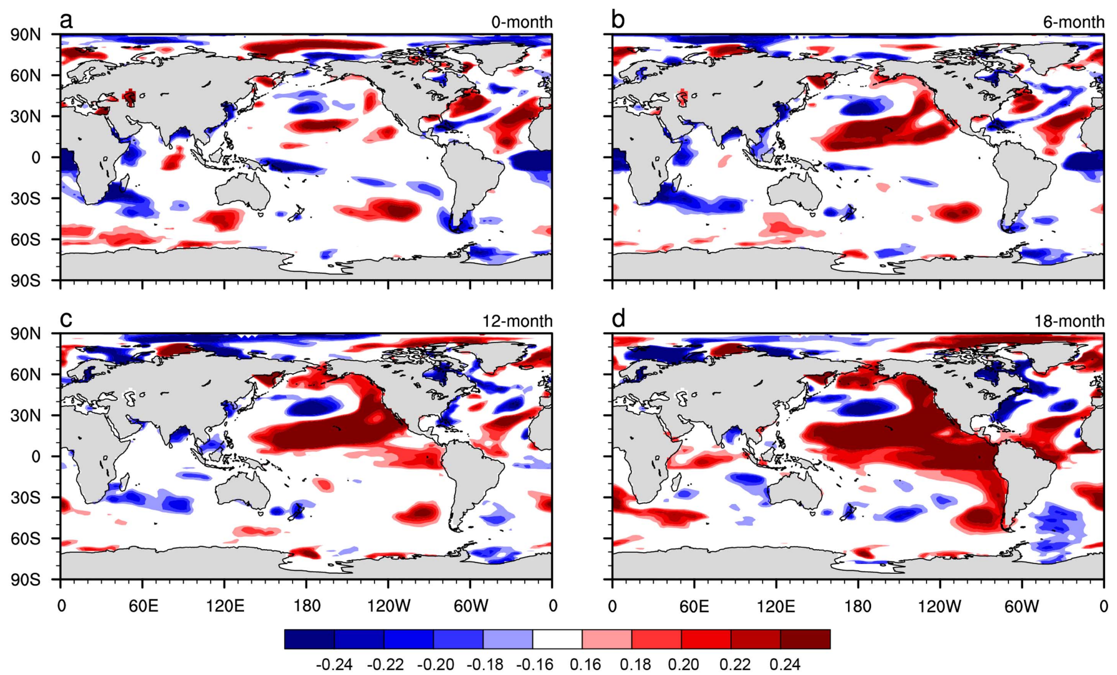

Figure 7. Correlation coefficients between the specified ASO×−1 and simulated SST for the period 1955–2005 in the model simulation experiments, E_1 (see table 1), when the ASO variations lead SST by (a) 0 months, (b) 3 months… and (h) 21 months. Ozone is specified from the CMIP5 ensemble mean ozone output. Simulated SST is as outputs from E_1. Only regions above the 95% confidence level are colored. Both specified ASO and simulated SST variations were detrended, and a 35 month low-pass filter was applied to ozone and SST.

et al 2012, Garfinkel *et al* 2015, Kren *et al* 2015, Woo *et al* 2015), and then affect polar ozone. The question arises whether the Northern Pacific SST variations drive the polar ozone and ENSO variations independently.

A historical experiment (E_1) covering the period 1955–2005 and with the specified ASO forcing applied to the CESM can capture the lagged effect of the specified ASO anomalies on the simulated ENSO (figure 7). Please see table 1 for a description of E_1. Focusing on

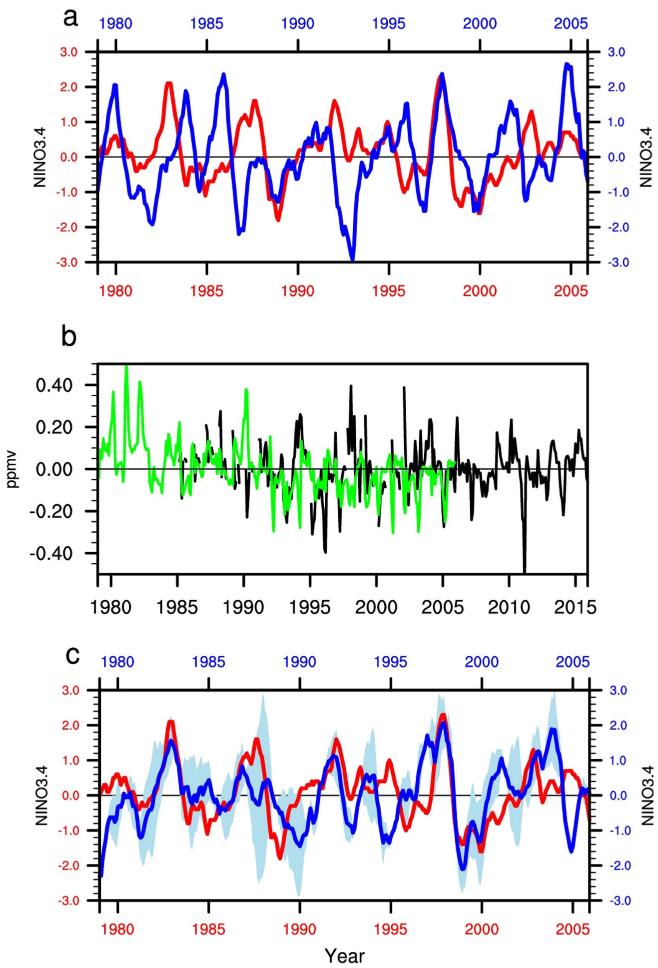

Figure 8. (a) ENSO index (red line) from the Climate Prediction Center/NOAA NINO3.4 index and the simulated ENSO index (blue) for the period 1985–2005. Simulated ENSO index is based on the SST outputs from E_1, in which the specified ASO forcing is from CMIP5's ozone output ensemble mean. (b) ASO variations from SWOOSH ozone (black line) and specified ASO forcing of E_1 (green line). (c) Same as (a), but the blue line indicates the simulated ENSO index based on the ensemble-mean SST outputs of $(E_2 + E_3 + E_4)/3$ (see table 1) in which the specified ASO forcing is from MERRA ozone. The light blue band represents the variation range of ensemble experiments.

the North and tropical Pacific, we find that the VM-like pattern appears over the North Pacific following the ASO anomaly (figure 7(a)) and is enhanced in the tropical Pacific after about 6–9 months (figure 7(b)). Finally, an El Niño-like event emerges one year later (figures 7(c) and (d)). This developmental sequence is similar to that observed (figure 6). Note that the ozone forcing is specified in the simulation; therefore, its variation should not be related to North Pacific SST anomalies.

Although the recent CMIP5 models can capture the spatial pattern of ENSO, there are large biases between simulated and observed ENSO variations (see Guilyardi *et al* 2009); for example, the ENSO index for the period 1979–2005 in E_1 which is a historical experiment simulated by CESM is not significantly correlated with the observed ENSO (figure 8(a); $r = 0.11$). Note that the specified ASO forcing in E_1 is derived from the CMIP5 ensemble mean ozone output, which is not in good agreement with the observed ozone variability (figure 8(b); $r = 0.14$). According to our results, ASO affects ENSO, so would improving the specified ASO forcing in simulations improve the simulated ENSO variations? The ASO from MERRA (1979–2015) was used as the specified ASO forcing in experiments E_2–E_4, because there are no missing values for ASO variations in MERRA and the data are in agreement with the observed ASO variations (figure 2). Interestingly, the correlation coefficient between the simulated ensemble-mean ENSO and observed ENSO variability is statistically significant (figure 8(c); $r = 0.42$), when MERRA ozone is used as the specified ASO forcing in the simulations. This result not only supports the impact of ASO on ENSO, but also implies that incorporating realistic ASO forcing in the model can improve the simulation of ENSO variability.

5. Discussion and conclusions

Previous studies have noted that the radiative effect of Antarctic stratospheric ozone (AASO) depletion (Solomon 1990, 1999, Ravishankara *et al* 1994, 2009)

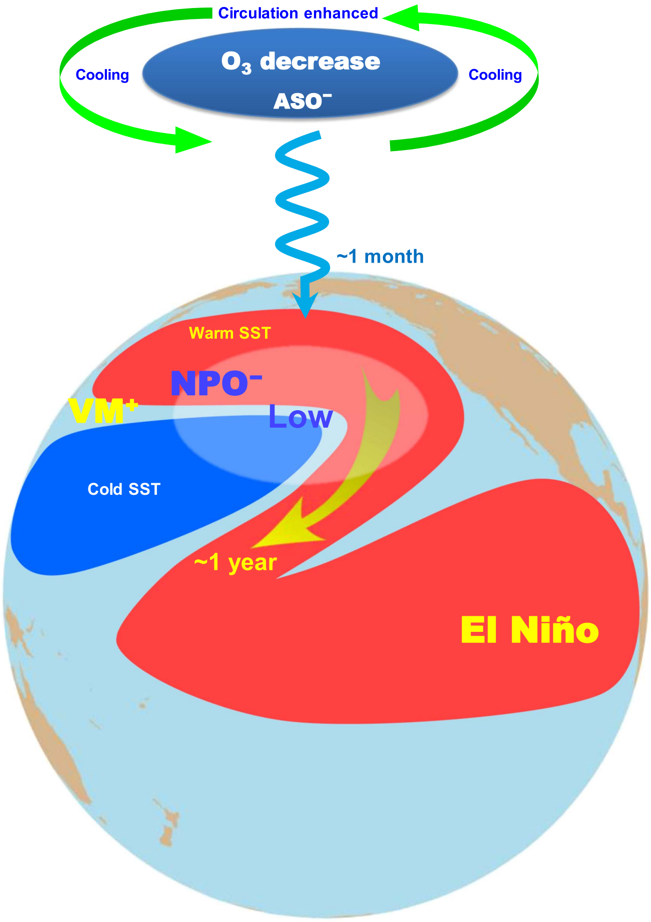

Figure 9. The two processes that combine to drive the ASO to El Niño connection: the high-latitude stratosphere to troposphere pathway (light blue wavy arrow) and the extratropical to tropical climate teleconnection (yellow curved arrow). ASO$^-$: Arctic stratospheric ozone decrease; NPO$^-$: Negative North Pacific Oscillation phase; VM$^+$: Positive Victoria Mode phase.

has a significant impact on the Southern Hemisphere tropospheric climate (Son *et al* 2008, Feldstein 2011, Kang *et al* 2011, Thompson *et al* 2011). In this study, we find that the AASO variations have no significant impact on ENSO (Not shown). This contrast between the influence of AASO and ASO anomalies on ENSO may be due to the lack of a robust teleconnection pathway from the Southern Hemisphere Pacific to the equatorial Pacific. It should be noted that the relatively warm water in the tropical North Pacific and the permanent northern Intertropical Convergence Zone serve as necessary anchors to allow the seasonal footprinting mechanism to operate in a geographically and seasonally favored manner. However, in the Southern Hemisphere Pacific, none of the equivalent anchors are of significance. This may explain why the influence of the AASO on ENSO is not significant.

Figure 9 summarizes our findings regarding the influence of the ASO on ENSO using a schematic illustration. A negative ASO anomaly cools the Arctic stratosphere, strengthening the stratospheric circulation. The downward propagation of a negative stratospheric geopotential height anomaly, which reaches the surface as a negative NPO anomaly in about one month, initiates a positive VM phase over the North Pacific. The evolution of the positive VM anomaly reaches the equatorial Pacific and strengthens an El Niño event when other conditions for its occurrence are ripe. The high-latitude stratosphere to troposphere pathway and the extratropical to tropical climate teleconnection take more than a year and a half. A positive ASO anomaly would have the opposite effect, and has the potential to strengthen a La Niña event via the same pathway. This impact of ASO on ENSO makes it a potentially useful predictor of ENSO events. It is well known that ENSO influences stratospheric ozone. This implies that there may be a two-way interaction

Table 2. Selection of strong El Niño, strong La Niña, and neutral events from 1985 to 2015. A strong El Niño/La Niña event is defined when the NINO3.4 index is greater than 1/less than −1; values between −1 and 1 represent a neutral event.

Strong El Niño	Strong La Niña	Neutral
1987	1988	The rest
1991	1998	
1997	1999	
2009	2007	
2015	2010	

or dynamic feedback between the ASO and ENSO. In even broader terms, understanding this kind of connection and potential feedback between the stratospheric tracer gases (such as ozone) and the climate system deserves more attention. Furthermore, the observed ENSO variability can be partly explained by simulated ENSO variability in CESM when an observed ASO forcing is used. This result reinforces the need for climate models to include fully coupled stratospheric dynamical–radiative–chemical processes if they are to more accurately simulate and predict future ENSO variations.

Acknowledgments

Funding for this project was provided by the Science Foundations of China (41225018, 2014CB441202, 41575039) and Youth Scholars Program of Beijing Normal University. We acknowledge the datasets from the MERRA, Climate Prediction Center/NOAA, SWOOSH, Hadley Centre, NCEP2, RICH. We thank NCAR for providing the CESM model. We also thank the helpful comments from Dr Bill Randel and Dr Mojib Latif on the study.

References

Ashok K and Yamagata T 2009 The El Niño with a difference *Nature* **461** 481–4

Baldwin M P and Dunkerton T J 2001 Stratospheric harbingers of anomalous weather regimes *Science* **294** 581–4

Bond N A, Overland J E, Spillane M and Stabeno P 2003 Recent shifts in the state of the North Pacific *Geophys. Res. Lett.* **30** 2183

Bretherton C S *et al* 1999 The effective number of spatial degrees of freedom of a time-varying field *J. Clim.* **12** 1990–2009

Brönnimann S, Luterbacher J, Staehelin J, Svendby T M, Hansen G and Svenøe T 2004 Extreme climate of the global troposphere and stratosphere 1940–1942 related to El Niño *Nature* **431** 971–4

Cagnazzo C and Manzini E 2009 Impact of the stratosphere on the Winter Tropospheric Teleconnections between ENSO and the North Atlantic and European Region *J. Clim.* **22** 1223–38

Cagnazzo C *et al* 2009 Northern winter stratospheric temperature and ozone responses to ENSO inferred from an ensemble of Chemistry Climate Models *Atmos. Chem. Phys.* **9** 8935–48

Calvo N, Polvani L M and Solomon S 2015 On the surface impact of Arctic stratospheric ozone extremes *Environ. Res. Lett.* **10** 094003

Calvo N *et al* 2004 Analysis of the ENSO signal in tropospheric and stratospheric temperatures observed by MSU, 1979–2000 *J. Clim.* **17** 3934–6

Camp C, Roulston M and Yung L 2003 Temporal and spatial patterns of the interannual variability of total ozone in the tropics *J. Geophys. Res.* **108** 4643

Charlton A J and Polvani L M 2007 A new look at stratospheric sudden warmings: I. Climatology and modeling benchmarks *J. Clim.* **20** 449–69

Chen S, Chen W, Yu B and Graf H F 2013 Modulation of the seasonal footprinting mechanism by the boreal spring Arctic Oscillation *Geophys. Res. Lett.* **40** 6384–9

Cheung J C H, Haigh J D and Jackson D R 2014 Impact of EOS MLS ozone data on medium-extended range ensemble forecasts *J. Geophys. Res.* **119** 9253–66

Chipperfield M P, Dhomse S S, Feng W, McKenzie R L, Velders G and Pyle J A 2015 Quantifying the ozone and ultraviolet benefits already achieved by the Montreal Protocol *Nat. Commun.* **6** 7233

Davis S M *et al* 2016 Stratospheric Water and Ozone Satellite Homogenized (SWOOSH) database: a long-term database for climate studies *Earth Syst. Sci. Data Discuss.* **8** 461–90

Deser C, Alexander M A, Xie S-P and Phillips A S 2010 Sea surface temperature variability: patterns and mechanisms *Annu. Rev. Mar. Sci.* **2** 115–43

Di Lorenzo E *et al* 2008 North Pacific Gyre Oscillation links ocean climate and ecosystem change *Geophys. Res. Lett.* **35** L08607

Ding R, Li J, Tseng Y H, Sun C and Guo Y 2015 The victoria mode in the North Pacific linking extratropical sea level pressure variations to ENSO *J. Geophys. Res.* **120** 27–45

Eyring V *et al* 2006 Assessment of temperature, trace species, and ozone in chemistry-climate model simulations of the recent past *J. Geophys. Res.* **111** D22308

Feldstein S B 2011 Subtropical rainfall and the Antarctic ozone hole *Science* **332** 925–6

Fischer A, Shindell D, Bourqui M, Faluvegi G, Rozanov E, Schraner M and Brönnimann S 2008 Stratospheric winter climate response to ENSO in three chemistry–climate models *Geophys. Res. Lett.* **35** L13819

Forster P and Shine K 1997 Radiative forcing and temperature trends from stratospheric ozone changes *J. Geophys. Res.* **102** 10841–55

Froidevaux L *et al* 2015 Global OZone Chemistry And Related trace gas Data records for the Stratosphere (GOZCARDS): methodology and sample results with a focus on HCl, H_2O, and O_3 *Atmos. Chem. Phys.* **15** 10471–507

Garfinkel C I and Hartmann D L 2008 Different ENSO teleconnections and their effects on the stratospheric polarvortex *J. Geophys. Res.* **113** D18114

Garfinkel C I, Hurwitz M M and Oman L D 2015 Effect of recent sea surface temperature trends on the Arctic stratospheric vortex *J. Geophys. Res.* **120** 5404–16

Gerber E P and Son S 2014 Quantifying the summertime response of the Austral Jet Stream and Hadley Cell to stratospheric ozone and greenhouse gases *J. Clim.* **27** 5538–59

Gettelman A, Randel W, Massie S and Wu F 2001 El Niño as a natural experiment for studying the tropical tropopause region *J. Clim.* **14** 3375–92

Graf H F and Walter K 2005 Polar vortex controls coupling of North Atlantic Ocean and atmosphere *Geophy. Res. Lett.* **32** L01704

Guilyardi E *et al* 2009 Understanding El Niño in ocean–atmosphere general circulation models: progress and challenges *Bull. Am. Meteorol. Soc.* **90** 325–40

Haigh J D 1994 The role of stratospheric ozone in modulating the solar radiative forcing of climate *Nature* **370** 544–6

Haimberger L, Tavolato C and Sperka S 2008 Towards elimination of the warm bias in historic radiosonde temperature records some new results from a comprehensive intercomparison of upper air data *J. Clim.* **21** 4587–606

Haynes P H, McIntyre M E, Shepherd T G, Marks C J and Shine K P 1991 On the 'downward control' of extratropical diabatic circulations by eddy-induced mean zonal forces *J. Atmos. Sci.* **48** 651–78

Hurwitz M M, Newman P A and Garfinkel C I 2012 On the influence of North Pacific sea surface temperature on the Arctic winter climate *J. Geophys. Res.* **117** D19

Hurwitz M M, Song I S, Oman L D, Newman P A, Molod A M, Frith S M and Nielsen J E 2011 Response of the Antarctic stratosphere to warm pool El Niño Events in the GEOS CCM *Atmos. Chem. Phys.* **11** 9659–69

Ineson S and Scaife A A 2009 The role of the stratosphere in the European climate response to El Niño *Nature Geosci.* **2** 32–6

Jadin E A, Wei K, Zyulyaeva Y A, Chen W and Wang L 2010 Stratospheric wave activity and the Pacific Decadal Oscillation *J. Atmos. Sol.-Terr. Phys.* **72** 1163–70

Jin F-F 1996 Tropical ocean-atmosphere interaction, the pacific cold tongue, and the El Niño Southern Oscillation *Science* **274** 76–8

Jin F-F 1997a An equatorial ocean recharge paradigm for ENSO: I. Conceptual model *J. Atmos. Sci.* **54** 811–29

Jin F-F 1997b An equatorial ocean recharge paradigm for ENSO: II. A stripped-down coupled model *J. Atmos. Sci.* **54** 830–47

Kang S M, Polvani L M, Fyfe J C and Sigmond M 2011 Impact of polar ozone depletion on subtropical precipitation *Science* **332** 951–4

Karpechko A, Yu A, Perlwitz J and Manzini E 2014 A model study of tropospheric impacts of the Arctic ozone depletion 2011 *J. Geophys. Res.* **119** 7999–8014

Kidston J, Scaife A, Hardiman S, Mitchell D, Butchart N, Baldwin M and Gray L 2015 Stratospheric influence on tropospheric jet streams, storm tracks and surface weather *Nat. Geosci.* **8** 433–40

Kren A C, Marsh D R, Smith A K and Pilewskie P 2015 Wintertime Northern Hemisphere response in the stratosphere to the Pacific Decadal Oscillation using the Whole Atmosphere Community Climate Model *J. Clim.* **29** 1031–49

Latif M and Keenlyside N S 2009 El Niño/Southern Oscillation response to global warming *Proc. Natl. Acad. Sci.* **106** 20578–83

Lean J, Rottman G, Harder J and Kopp G 2005 SORCE contributions to new understanding of global change and solar variability *Sol. Phys.* **230** 27–53

Li J P, Sun C and Jin F-F 2013 NAO implicated as a predictor of Northern Hemisphere mean temperature multidecadal variability *Geophys. Res. Lett.* **40** 5497–502

Li Y, Li J P and Feng J 2012 A teleconnection between the reduction of rainfall in southwest western Australia and North China *J. Clim.* **25** 8444–61

Lubin D and Jensen E H 2002 Effects of clouds and stratospheric ozone depletion on ultraviolet radiation trends *Nature* **377** 710–3

Manney G L *et al* 2011 Unprecedented Arctic ozone loss in 2011 *Nature* **478** 469–75

Manzini E, Giorgetta M A, Esch M, Kornblueh L and Roeckner E 2006 The influence of sea surface temperatures on the Northern winter stratosphere: ensemble simulations with the MAECHAM5 Model *J. Clim.* **19** 3863–81

Marsh D R, Mills M J, Kinnison D E, Lamarque J-F, Calvo N and Polvani L M 2013 Climate change from 1850 to 2005 simulated in CESM1 (WACCM) *J. Clim.* **26** 7372–91

McPhaden M J, Zebiak S E and Glantz M H 2006 ENSO as an integrating concept in earth science *Science* **314** 1740–5

Orlove B S, Chiang J C H and Cane M A 2000 Forecasting Andean rainfall and crop yield from the influence of El Niño on Pleiades visibility *Nature* **403** 68–71

Ramaswamy V, Schwarzkopf M D and Randel W J 1996 Fingerprint of ozone depletion in the spatial and temporal pattern of recent lower-stratospheric cooling *Nature* **382** 616–8

Randel W, Garcia R, Calvo N and Marsh D 2009 ENSO influence on zonal mean temperature and ozone in the tropical lower stratosphere *Geophys. Res. Lett.* **36** L15822

Randel W J 1988 The seasonal evolution of planetary waves in the southern hemisphere stratosphere and troposphere *Q. J. R. Meteorol. Soc.* **114** 1385–409

Ravishankara A R, Daniel J S and Portmann R W 2009 Nitrous oxide (N_2O): the dominant ozone-depleting substance emitted in the 21st century *Science* **326** 123–5

Ravishankara A R *et al* 1994 Do hydrofluorocarbons destroy stratospheric ozone *Science* **263** 71–5

Reichler T, Kim J, Manzini E and Kroger J 2012 A stratospheric connection to Atlantic climate variability *Nat. Geosci.* **5** 783–7

Smith K L and Polvani L M 2014 The surface impacts of Arctic stratospheric ozone anomalies *Environ. Res. Lett.* **9** 074015

Solomon S 1990 Antarctic ozone: progress towards a quantitative understanding *Nature* **347** 347–54

Solomon S 1999 Stratospheric ozone depletion: a review of concepts and history *Rev. Geophys.* **37** 275–316

Son S-W *et al* 2008 The impact of stratospheric ozone recovery on the Southern Hemisphere westerly jet *Science* **320** 1486–9

Thompson D W J and Solomon S 2005 Recent stratospheric climate trends as evidenced in radiosonde data: global structure and tropospheric linkages *J. Clim.* **18** 4785–95

Thompson D W J *et al* 2011 Signatures of the Antarctic ozone hole in Southern Hemisphere surface climate change *Nat. Geosci* **4** 741–9

Timmermann A, Oberhuber J, Bacher A, Esch M, Latif M and Roeckner E 1999 Increased El Niño frequency in a climate model forced by future greenhouse warming *Nature* **398** 694–7

Vimont D J, Battisti D S and Hirst A C 2001 Footprinting: a seasonal connection between the tropics and mid-latitudes *Geophys. Res. Lett.* **28** 3923–6

Waugh D W, Garfinkel C I and Polvani L M 2015 Drivers of the recent tropical expansion in the Southern Hemisphere: changing SSTs or Ozone Depletion *J. Clim.* **28** 6581–6

Woo S H, Sung M K, Son S W and Kug J S 2015 Connection between weak stratospheric vortex events and the Pacific Decadal Oscillation *Clim. Dyn.* **45** 3481–92

World Meteorological Organization (WMO) 2011 Scientific assessment of ozone depletion: 2010 *Technical Report, Global Ozone Research and Monitoring Project Report No.* 52 Geneva, Switzerland p 516

Xie F, Li J P, Tian W S, Feng J and Huo Y 2012 The signals of El Niño Modoki in the tropical tropopause layer and stratosphere *Atmos. Chem. Phys.* **12** 5259–73

Xie F, Li J P, Tian W S and Zhang J K 2014 The relative impacts of El Niño Modoki, Canonical El Niño, and QBO on tropical ozone changes since the 1980s *Environ. Res. Lett.* **9** 064020

Yeh S, Kug J, Dewitte B, Kwon M, Kirtman B and Jin F-F 2009 El Niño in a changing climate *Nature* **461** 511–4

Zhang J, Tian W, Wang Z, Xie F and Wang F 2015 The influence of ENSO on Northern mid-latitude ozone during the winter to spring transition *J. Clim.* **28** 4774–93

Zhang J, Tian W S, Chipperfield M P, Xie F and Huang J 2016 Persistent shift of the Arctic polar vortex towards the Eurasian continent in recent decades *Nat. Clim. Change* **6** 1094–9